Geomagnetism and Aeronomy, Vol. 42, No. 4, 2002, pp. 467–473. Translated from Geomagnetizm i Aeronomiya, Vol. 42, No. 4, 2002, pp. 491–498.
Original Russian Text Copyright © 2002 by Afraimovich, Kosogorov, Leonovich, Pirog.
English Translation Copyright © 2002 by МАИК "Наука/Interperiodica" (Russia).

Global Pattern of Large-Scale Ionospheric Disturbances during the Magnetic Storm of September 25, 1998, as Inferred from GPS Network Data

E. L. Afraimovich, E. A. Kosogorov, L. A. Leonovich, and O. M. Pirog

Institute of Solar–Terrestrial Physics, Siberian Division, Russian Academy of Sciences, P.O. Box 4026, Irkutsk, 664033 Russia

e-mail: afra@iszf.irk.ru, e-mail: pir@iszf,irk.ru

Received January 11, 2001; in final form, March 22, 2001

Abstract—The results of studying ionospheric effects of the large magnetic storm of September 25, 1998, based on an analysis of the global maps of total electron content (TEC) constructed using GPS network data, have been presented. The most pronounced consequence of the magnetic storm shown in the TEC maps includes prolonged negative disturbances extending to geographic latitudes of lower than 30° N, disappearance of the equatorial minimum, and displacement of the main maximum to morning hours at the phase of storm recovery. The TEC response to the magnetic storm depends on the local time of its commencement, which results in a clearly defined longitudinal effect. In the European sector, the δTEC variations change their sign with a period of about a day, and the positive and negative phases are observed in daytime and at night, respectively. At the same time, over North America, the positive phase appears only at night, the negative phase is observed in daytime, and the negative disturbances are observed during the entire period of observation at latitude from 30° to 60° N. The latitudinal effect is also significant. The maximal positive variations (to 100% and more) were observed in the equatorial region and at high latitudes. The δTEC variations have a quasi-wavy character with a period of about one day, which is possibly related to the propagation of large-scale ionospheric disturbances.

1. INTRODUCTION

An ionospheric storm manifests itself as a global disturbance of the total electron content (TEC), electron density at the F region maximum (N_mF2), and maximum altitude during a geomagnetic storm as a result of different dynamic and chemical processes. Owing to the complex of different processes interacting in the magnetosphere–ionosphere–thermosphere system, each storm is individual and a prediction of its behavior is still an art rather than a science. The state of the ionosphere during a storm depends on many variables such as LT, observation-point coordinates, season, solar activity phase, storm commencement time, storm duration, disturbance value, and prestorm activity (large storms are rarely isolated). Moreover, the physics controlling the global ionosphere and atmosphere is complicated by the fact that geomagnetic disturbances are insufficiently predictable.

A low space–time resolution of the available methods for diagnosing the ionosphere is one of the main factors hindering the formation of a reliable pattern of the ionospheric response to geomagnetic disturbances. The main volume of information was obtained at the network of ionosondes [Matsushita, 1959; Prollss *et al.*, 1991; Wrenn *et al.*, 1987]. The global response to the magnetic storm was studied by Pulinets *et al.* [1996], Szuszczewicz *et al.* [1998], and Yeh *et al.* [1994]. They observed prolonged negative disturbances that propagated from middle to low latitudes during the main phase maximum and caused a temporal suppression of the equatorial anomaly. Depending on the local time of a storm sudden commencement (SSC), the ionospheric response was different at different longitude sectors, which resulted in the longitudinal effect. Several publications were devoted to the use of TEC measurements of UHF signals of geostationary satellites, which can ensure monitoring of the ionosphere, in studies of ionospheric storms [Essex *et al.*, 1981]. A serious disadvantage of similar methods is the too small and progressively decreasing number of such geostationary satellites and their irregular distribution in longitude. The development of the global positioning system (GPS) and the creation (on its basis) of a widely branched international service (IGS), which included about 500 GPS receivers at the beginning of 1999 according to Internet data, open a new era in the remote diagnostics of the ionosphere. The use of the network of GPS receivers for studying the ionosphere has several advantages over more traditional methods: (1) simultaneous global coverage, (2) high resolution in time, (3) continuous measurements, and (4) data availability. Thus, TEC measurement is a powerful new method for studying and monitoring the processes of development of an ionospheric storm.

In the last few years, several researchers [Manucci *et al.*, 1998; Schaer *et al.*, 1998] have created a new technology for constructing global maps of the absolute vertical TEC value using the data of the IGS–GPS network (the Global Ionospheric Map (GIM) technology). The GIM technology, along with the possibility of obtaining these maps in the IONEX standard format from the Internet, have given researchers a new powerful tool for studying large-scale ionospheric processes under quiet and disturbed conditions on a global scale. Such new data on the global development of large-scale ionospheric disturbances during large ionospheric storms, previously unobtainable from the data of traditional measurements with the help of ionosondes or even incoherent scatter radars [Ho *et al.*, 1998; Jakowski *et al.*, 1999], were obtained with the use of this technology.

We present results of studying ionospheric effects of the large magnetic storm of September 25, 1998, based on an analysis of the global TEC maps in the IONEX format, constructed at a 2-h interval using the IGS–GPS data. We also used the special procedure for normalizing TEC maps to background conditions (which makes it possible to distinguish a disturbed part of the global time distribution of TEC) developed by Ho *et al.* [1998].

2. DESCRIPTION OF GEOMAGNETIC CONDITIONS AND DATA ANALYSIS

The large storm with a maximal amplitude of 233 nT was observed in *Dst* variations on September 25, 1998. The *Kp* indices at the storm maximum reached values of eight, and the daily sum of *Kp* was 48 on September 25. Unfortunately, this storm developed against a rather disturbed background: on September 24 the sum of *Kp* was 29 and the *Dst* variation values were about –50 nT. At 0100 UT the *Dst* variation sharply increased to zero, then began to rapidly decrease, and became equal to –220 and –233 nT at 0700 and 1000 UT, respectively. Then the recovery phase began and continued to September 30. We have analyzed global variations in the total electron content in the Northern Hemisphere during the storm and at the phase of its recovery in the period of September 24–27. September 20 was taken as a quiet day (a reference level) in the calculations (the *Kp* daily sum was equal to nine). Figure 1 presents the maps of the TEC global distribution on September 20 and 24–27 in geographic coordinates at selected UT instants. The TEC global distribution at a quiet time (*Kp* = 1) is shown in Fig. 1a (at 1100 UT on September 20). The map clearly indicates a daytime maximum, which is more pronounced at latitudes lower than 40°, moves from 1100–1200 LT at high latitudes to 1500 LT below 40°, and has maximal values (more than 70 TECU) at latitudes lower than 20°. Two regions of low (lower than 10 TECU) values are distinguished in night and predawn hours: the main ionospheric trough at high latitudes and the equatorial minimum at low latitudes. We should note that the TEC values in the main ionospheric trough and the equatorial minimum are of the same order of magnitude. At high and middle latitudes the ratio of the TEC daytime and nighttime values is equal to two to two and a half, increases with decreasing latitude, and is about eight near the equator.

At increasing *Kp* on September 24 (Fig. 1b), the form of the TEC distribution barely changes, but at night the high-latitude region of low TEC values widen in longitude and shift toward the equator. In the daytime sector, the TEC values decrease at high latitudes and increase at low ones. The maximum (crest of the equatorial anomaly) is clearly defined near 20°. At the phase of storm expansion at 0300 UT on September 25 (*Kp* = 8), the equatorial minimum disappears at night and the crest of the equatorial anomaly near 20° becomes more pronounced in the daytime sector (Fig. 1c). At the storm maximum at 1100 UT (Fig. 1d), the region of low TEC values (lower than 10 TECU) in the nighttime sector extends to latitudes lower than 20°. In daytime hours, the TEC decreases from high to low latitudes and the crest of the equatorial anomaly shifts toward the equator. At the phase of storm recovery (Fig. 1e), the TEC values continue decreasing and at 2100 UT become twice lower at all latitudes. At the same time, the daytime peak disappears and two maximums are observed in the TEC daily variation near the equator: in the dawn sector (0700–0900 LT) and about 1500 LT. In the nighttime sector, the polar wall of the main ionospheric trough is insufficiently pronounced and after midnight the region of low TEC values extends from 80° to the equator (Fig. 1f). On the subsequent days, the recovery is very slow, though *Kp* decreases to one to two. On September 26, the equatorial boundary of low TEC values remains at a level of 40° and the polar boundary is still insufficiently pronounced. The minimum is seen near the equator in predawn hours. The maximum in the TEC diurnal variation is observed in the dawn hours, since the daily ionization remains very low (Fig. 1g). One day later (Fig. 1h), the maximum in the TEC diurnal variations at low latitudes returns to its previous position, the main ionospheric trough acquires a more distinct structure, and its polar wall shifts toward the calculated level. The predawn equatorial minimum retains its position, and he ionization level in the auroral zone remains rather low in all maps.

The changes in the state of the ionosphere are more evident in the variations in the disturbance index. This index represents a ratio of the difference between TEC values during disturbances and at a quiet time to an undisturbed value, in percent [Ho *et al.*, 1998].

$$\delta\mathrm{TEC} = (\mathrm{TEC_d} - \mathrm{TEC_q})/\mathrm{TEC_q} \times 100\%.$$

Figure 2 presents variations in the disturbance index on September 24–27 at opposite meridians (30° and 210°) averaged over a latitude interval of 10°. The observed disturbances differ in both latitude and longitude.

At a latitude of 30°, the storm commencement and its main phase are observed at night and in the morning and the *Dst* variations are maximal at noon. Insignifi-

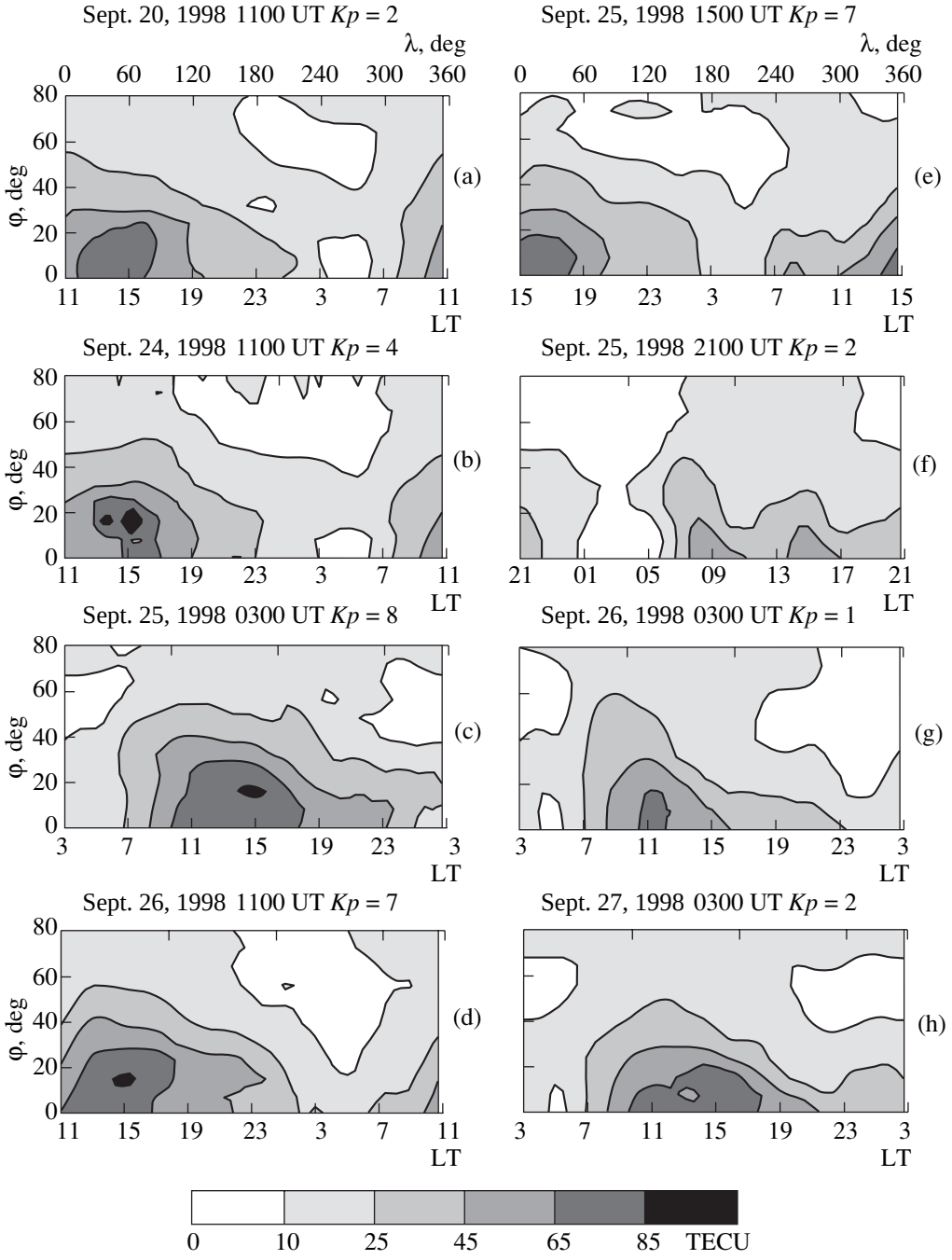

Fig. 1. Maps of the TEC global distribution in geographic coordinates in the Northern Hemisphere at the following selected instants: (a) quiet time; (b) before the storm; (c)–(f) during the storm; (g) and (h) after the storm.

cant disturbances at high (higher than 60°) and low (lower than 30°) latitudes occur at the beginning of the storm. The lower latitude, the higher the *Dst* variation. At the storm maximum and recovery phase, negative disturbances with an amplitude of above 40% are observed at latitudes higher than 50°, whereas at lower latitudes, the disturbances are positive and have an amplitude of up to 50%. We should note that on the day of the storm and on the following days, the wavelike alternation of positive and negative δTEC values with a quasiperiod of about a day is most pronounced at latitudes of 40°–70°. The wave phase is positive in daytime and negative at night. North of 70° and south of 40°, the fluctuations with smaller periods are superimposed on the main wave. On September 27, the fluctuation amplitude is insignificant at mid-latitudes (30°–50°).

At λ = 210°, the storm commencement is observed in the afternoon. Even before the storm of September 24, the TEC increases by 30–40% at high latitudes and by about 100% at low latitudes at a nighttime increase in

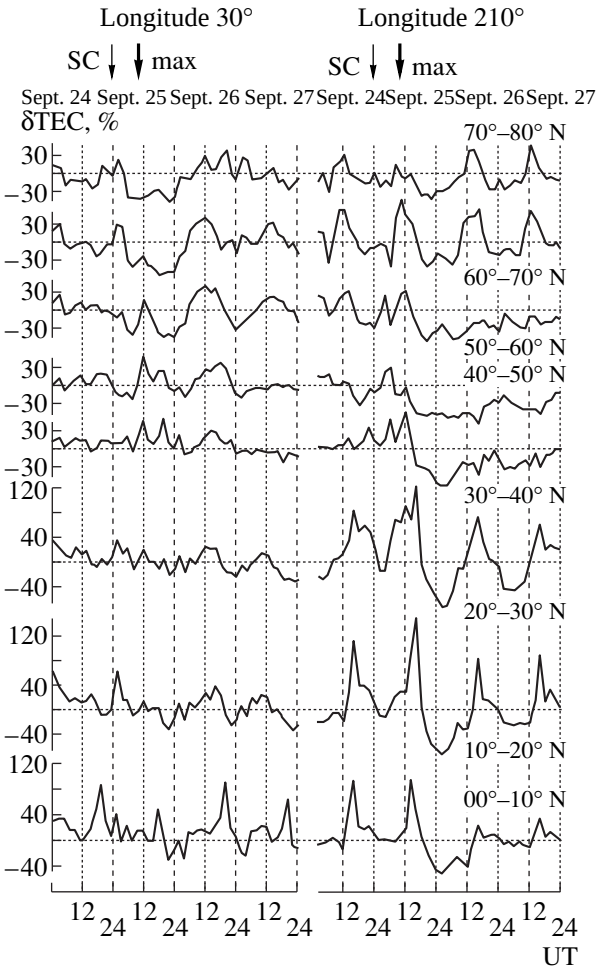

Fig. 2. Variations in the δTEC disturbance index on September 24–27 at opposite meridians (30° and 210° E) averaged in a latitude interval of 10°. Arrows on the time axis indicate the instants of the SSC and the *Dst* maximum. Vertical dashed and solid lines show local midnight and midday, respectively.

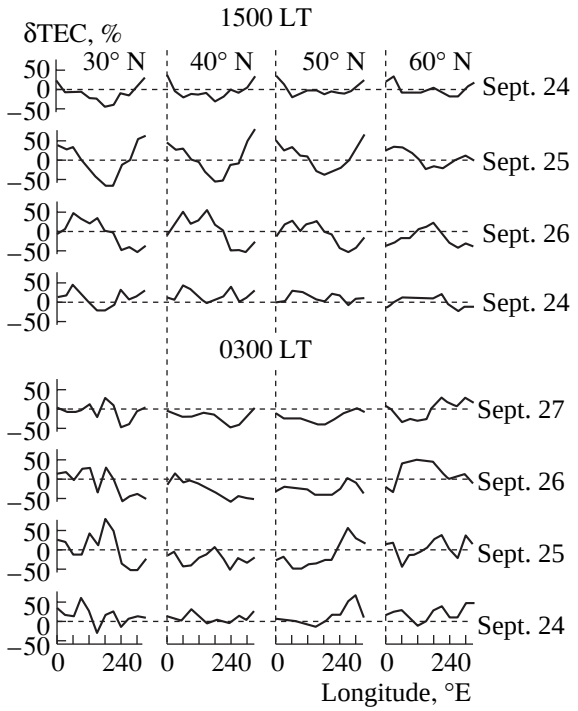

Fig. 3. Longitudinal variations in the δTEC disturbance index at different latitudes for daytime (1500 LT) and nighttime (0300 LT) hours.

Kp to five, which is also shown in the TEC maps. During the storm main phase and at its maximum intense positive, disturbances are observed in the dusk and nighttime sectors from the equator to the auroral zone after insignificant (less than 30%) negative deviations. The negative phase in the TEC variations in this longitude sector appears in daytime and lasts for more than two days at latitudes from 30° to 60°. North of 60° and south of 30°, the positive phase is observed at night. Both phases mainly exceed 50%, but negative deviations are less intense at lower latitudes. As at a longitude of 30°, the δTEC variations have a wavelike character, a period of about a day, and are superimposed on the main wave of fluctuations with smaller periods.

Figure 3 indicates the δTEC longitude variations at latitudes of 30°–60° for daytime (1500 LT) and nighttime (0300 LT) hours. South of 30° and north of 60°, the variations are not shown because of their rather chaotic character and large amplitudes. In the daytime of September 24, the δTEC variations are wavy with positive phase maximums at longitudes of 60° and 240° and at all latitudes. The negative phase is less significant, is observed between these longitudes, and has a maximum at 150°–180°. The disturbance amplitude decreases with increasing latitude. On the most disturbed day (September 25), the negative disturbances are observed mostly at longitudes of 200°–360° in the Western Hemisphere and have a maximal deviation of about 60% at 270°–300°. Positive disturbances with an amplitude of up to 50% are observed at latitudes of 30°–50° in the eastern sector. On the following day, the negative phase is observed at longitudes of 120°–240° with the maximal deviation at 180°. The amplitude of these disturbances changes from 30 to 70% with decreasing latitude. The positive phase has a maximum (about 60%) at 330°. On the second day after the storm (September 27), the amplitudes of negative disturbances exceed 40% only at a latitude of 30° and are insignificant at higher and lower latitudes. At high latitudes (60°), a negative δTEC with amplitudes of up to 50% predominate on the day of the storm, and the sign of disturbances reverses on the following day. The positive disturbances are maximal (50%) at $\lambda = 60°$. We assume that the wave that originated on the day of the storm propagates along the parallel and from high latitudes toward the equator, and that the amplitude of its negative phase increases. The point of disturbance sign reversal on the following days shifts toward lower longitudes.

At night, the differences in latitudes and longitudes are more considerable and are difficult to describe. At a latitude of 30°, the δTEC variations are similar on all days of observations but are more intense on the day of the storm. The positive disturbances have a maximum of higher than 60% at longitudes of 180°–210°. Considerable negative disturbances (up to 50%) appear at a latitude of 30° at longitudes of 270°–300° on the day of the storm and on the following day.

Beginning with September 24, negative disturbances with an amplitude of up to 60% predominate at a latitude of 40° at all longitudes. Positive δTEC are significant at a latitude of 50° in the longitude region 250°–310°. At high latitudes (60°), the δTEC variations are most intense on the following day after the storm. The negative disturbances have a maximum at a longitude of 60°, and the positive phase with a maximum of higher than 50% is observed at longitudes of 60°–240°.

Figure 4 presents a generalized pattern of TEC variations in UT coordinates and longitude at latitudes of 30°–60°. North of 70° and south of 30°, we could not draw an integral pattern because of the lack of data. Dashed lines show local midnight; solid lines, midday; and arrows on the vertical axis, the instants of the storm commencement and maximal *Dst* values. Figure 4 indicates that both positive and negative disturbances are hardly higher than 30% before the storm on September 24. The areas with increased TEC are observed only near midnight at latitudes of 50°–60° in the longitude range of 200°–330°, and positive disturbances are observed before the storm at a latitude of 30° at all longitudes.

During the storm commencement and the main-phase positive disturbances, the region of which is bounded by the line of midnight, outside which the disturbances change their sign, are observed at middle and low latitudes in the Eastern Hemisphere. The lower the latitude, the more western the boundary of propagation of the positive phase. Negative disturbances predominate in the Western Hemisphere during all days under study except for small regions of positive disturbances in daytime hours.

At high latitudes (50°–70°), negative disturbances predominate on the day of the storm and positive δTEC are observed near midnight at longitudes of 210°–240°. On the following days, the positive phase appears in daytime hours near Greenwich meridian and propagates to all longitudes with increasing latitude. The disturbances change their sign with a periodicity of one to one and a half days.

3. DISCUSSION

The analysis performed makes it possible to distinguish several main features of the TEC response to the storm. Before the storm, positive disturbances, probably caused by the widening of the zone of auroral ionization and by the disappearance of the equatorial minimum, are observed in nighttime hours at high latitudes and near the equator (Fig. 1). It is important to note that the TEC values in the regions of the main ionospheric trough and the equatorial minimum are close. At the phase of storm recovery, the trough equatorial wall is absent and the zone of low ionization extends from high latitudes to the equator (Fig. 1f). A similar effect has been detected in the data of topside sounding from the Intercosmos-19 satellite [Indyukov *et al.*, 1985]. This effect can be explained by the fact that after a strong storm, the plasmasphere empties and the nighttime ionosphere is not sustained by fluxes from it. As a result, electron density values remain very low. In the quiet period, a trough equatorial wall appeared and gradually displaced to higher latitudes as the plasmasphere was filled. A similar pattern was also observed in the GPS data (Figs. 1g, 1h).

On the day of the storm, the ionospheric behavior is different at different longitudes, which possibly depends on the local time of the storm commencement. At longitudes where the storm starts after midnight and in the dawn sector, the negative phase, which becomes positive in daytime hours and negative again at night, begins after the positive disturbance in nighttime hours. In the regions where the storm appears in dusk hours, the nighttime positive disturbance changes into the daytime negative disturbance and such an alternation remains at high and low latitudes; at mid-latitudes, the negative phase lasts up to the final storm recovery (Fig. 2). Similar variations were observed by Yeh *et al.* [1994], who assumed that the longitudinal effects are caused by the local time of an SSC and by different mechanisms operating at different longitudes.

The most pronounced effect is global decreases in the TEC. They cover all latitudes and most longitudes and are observed at the phases of storm expansion and recovery. At middle and high latitudes in the western sector, the zone of negative δTEC values covers a time interval longer than 36 h. These values are typical of negative effects caused by changes in the neutral composition [Prollss *et al.*, 1991; Szuszczewicz *et al.*, 1998; Wrenn *et al.*, 1987]. The negative disturbances observed in dusk and nighttime hours in the European sector are possibly related to the equatorward shift of the main ionospheric trough [Eliseev *et al.*, 1995].

Prolonged (to 12 h) intense positive disturbances were observed in daytime hours over Europe. Similar disturbances have been studied by Bauske and Prollss [1998] and Jakowski *et al.* [1999]. The conclusion has been drawn that for positive ionospheric storms, wind disturbances are more important than changes in composition. Moreover, certain features in TEC variations over Europe testify to the action of eastward electric fields during the storm's initial phase.

The quasiperiodic structure of the variations observed in Figs. 2–4 leads us to the conclusion that wave processes should play an important role in storm effects. Deminov and Karpachev [1985] established that large-scale internal gravity waves are generated by

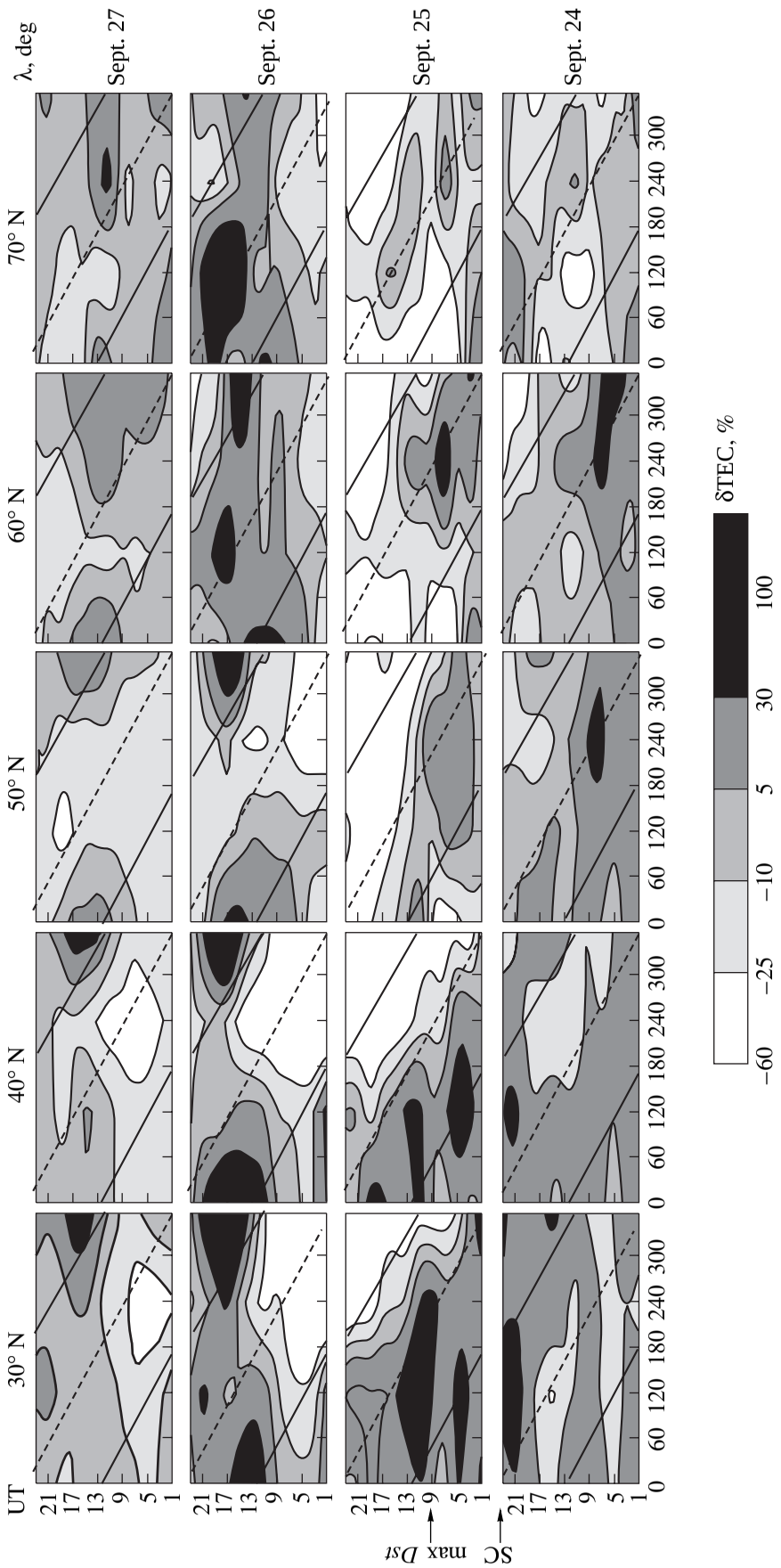

Fig. 4. The dynamics of the δTEC longitudinal variations at different latitudes. The time increases from bottom to top. Arrows on the left-hand vertical axis indicate the instants of the storm commencement and activity maximum. Dashed and solid lines show local midnight and midday, respectively.

auroral electrojets during their sharp enhancement in the course of magnetospheric disturbances and then propagate from auroral latitudes to lower ones over large distances (of about several thousand kilometers). Since in this paper we did not consider large-scale structure, it is difficult to determine disturbance propagation velocity using the data presented. However, the propagation direction from high to low latitudes and from east to west is clearly traced. Deminov and Karpachev [1985], Essex *et al.* [1981], and Shashun'kina *et al.* [1998] observed similar regularities.

4. CONCLUSIONS

The results of observations lead us to the following conclusions:

(1) The widening of the zone of low ionization to a geographical latitude of 40° and the displacement of the daytime maximum to dawn hours are the most pronounced consequence of the magnetic storm in the TEC maps.

(2) The storm negative phase is the main characteristic and is most intense at the storm recovery phase.

(3) The TEC values in the statistical regions of the main ionospheric trough and equatorial minimum are close. At the phase of storm recovery, the equatorial wall of the trough disappears after midnight, which results in very low TEC values from high latitudes to the equator.

(4) The TEC response to the magnetic storm depends on the local time of its commencement, which leads to the clearly defined longitudinal effect. In the European sector, the δTEC variations change their sign with a period of about a day and the positive and negative phases are observed in daytime and at night, respectively. Over North America, on the contrary, the positive phase appears only at night, the negative phase is observed in daytime hours, and the negative disturbances occur in the entire period of observations at latitudes of 30°–60°.

(5) The latitudinal effect is also significant. The maximal positive variations (to 100% and higher) were observed in the equatorial region and at high latitudes.

(6) The δTEC variations have a quasi-wavy character with a period of about one days. The change of the phase sign shifts from east to west with increasing distance from the storm main phase. A comparison with the data obtained by other researchers corroborates the thesis that ionospheric effects are different for different storms. There are general regularities in the type of the global negative disturbance and the alternation of the negative and positive phases, but the details, time of observation, duration, etc., are different and depend on many factors, which are very difficult to take into account.

ACKNOWLEDGMENTS

We are grateful to A.V. Tashchilin for interest to this work and useful pieces of advice.

This work was supported by the leading scientific schools of the Russian Federation (grant no. 00-15-98509) and the Russian Foundation for Basic Research (project nos. 00-05-72026 and 01-05-65374).

REFERENCES

Bauske, R. and Prolls, G.W., Numerical Simulations of Long-Duration Positive Ionosperic Storm Effects, *Adv. Space Res.*, 1998, vol. 22, pp. 117–121.

Deminov, M.G. and Karpachev, A.T., Ionospheric Response to a Magnetospheric Storm, *Prognozirovanie ionosfery i uslovii rasprostraneniya radiovoln* (Prediction of the Ionosphere and Radiowave Propagation Conditions), Moscow: Nauka, 1985, pp. 68–77.

Eliseev, A.Yu., Besprozvannaya, A.S., and Shchuka, T.I., Empirical Modeling of the Ionosphere Behavior during Global Magnetic Storms, *Geomagn. Aeron.*, 1995, vol. 35, no. 1, pp. 148–141.

Essex, E.A., Mendillo, M., Schodel, J.P., *et al.*, A Global Response of the Total Electron of the Ionosphere to the Magnetic Storm of 17 and 18 June 1972, *J. Atmos. Terr. Phys.*, 1981, vol. 43, pp. 293–306.

Ho, C.M., Mammucci, A.J., Sparks, L., *et al.*, Ionospheric Total Electron Content Perturbations Monitored by the GPS Global Network during Two Northern Hemisphere Winter Storms, *J. Geophys. Res.*, 1998, vol. 103, pp. 26 409–26 420.

Indyukov, A.E., Klimov, N.N., Vasil'eva, G.V., and Fligel', M.D., Position of the Main Ionospheric Trough as Inferred from the Data of Topside Sounding, *Issled. Geomagn. Aeron. Fiz. Solntsa*, 1985, no. 71, pp. 58–61.

Jakowski, N., Schlutter, S., and Sardon, E., Total Electron Content of the Ionosphere during the Geomagnetic Storm on 10 January, 1997, *J. Atmos. Solar–Terr. Phys.*, 1999, vol. 61, pp. 299–305.

Mannucci, A.J., Ho, C.M., Lindqwister, U.J., *et al.*, A Global Mapping Technique for GPS-Derived Ionospheric TEC Measurements, *Radio Sci.*, 1998, vol. 33, pp. 565–570.

Matsushita, S., A Study of the Morphology of Ionospheric Storms, *J. Geophys. Res.*, 1959, vol. 64, pp. 305–321.

Prolls, G.W., Brace, L.H., Mayer, H.G., *et al.*, Ionospheric Storm Effects at Subauroral Latitudes: A Case Study, *J. Geophys. Res.*, 1991, vol. 96, no. 2, pp. 1275–1288.

Pulinets, S.A., Yudakhin, K.F., and Evans, D., Study of the Ionosperic Variability within the Euro–Asian Sector during the Sundial/Atlas 1 Mission, *J. Geophys. Res.*, 1996, vol. 101, pp. 26 759–26 767.

Schaer, S., Gurtner, W., and Feltens, J., IONEX: The Ionosphere Map Exchange Format Version 1, *Proc. IGS AC Workshop*, Darmstadt, 1998, pp. 233–247.

Shashun'kina, V.M., Deminova, G.F., and Goncharova, E.E., Simulation of the Global VGV Effect in the Nighttime Ionosphere, *Geomagn. Aeron.*, 1998, vol. 38, no. 1, pp. 56–71.

Szuszczewicz, E.P., Lester, M.P., Wilkinson, P., *et al.*, A Comparative Study of Global Ionosperic Responses to Intense Magnetic Storm Conditions, *J. Geophys. Res.*, 1998, vol. 103, pp. 11 605–11 684.

Wrenn, G.L., Rodger, A.S., and Rishbeth, H., Geomagnetic Storms in the Antarctic *F*-Region. 1. Diurnal and Seasonal Patterns for Main Phase Effects, *J. Atmos. Solar–Terr. Phys.*, 1987, vol. 49, pp. 901–913.

Yeh, K.C., Ma, S.Y., Lin, K.H., *et al.*, Global Ionospheric Effects of the October 1989 Geomagnetic Storm, *J. Geophys. Res.*, 1994, vol. 99, pp. 6201–6218.